Electronic Supplementary Material (ESI) for Energy & Environmental Science.
This journal is © The Royal Society of Chemistry 2016

Supporting Information

Optical resonance and charge transfer behavior on patterned WO_3 microdisc arrays

Hye Won Jeong,[1,2] Weon-Sik Chae,[3] Bokyung Song,[4] Chang-Hee Cho,[4] Seong-Ho Baek,[5] Yiseul Park[5,*] and Hyunwoong Park[1,2,*]

[1]School of Energy Engineering and [2]School of Architectural, Civil, Environmental, and Energy Engineering, Kyungpook National University, Daegu 41566, Korea
[3]Analysis Research Division, Daegu Center, Korea Basic Science Institute, Daegu 41566, Korea
[4]Department of Emerging Materials Science and [5]Division of Nano and Energy Convergence Research, DGIST, Daegu 42988, Korea

*To whom correspondence should be addressed:

E-mail: dewpark@dgist.ac.kr (Y.P.); hwp@knu.ac.kr (H.P.)

Table S1. Time-resolved photoluminescence (TRPL) emission decay time and abundance of samples for full, green, and blue emission spectra.

		Film			Disc	
Full emission	τ (ns)	0.045	0.251	1.876	0.044	0.332
	Abundance (%)	57.3	42.1	0.6	78.8	21.2
Green Emission	τ (ns)	0.045	0.254	1.819	0.044	0.255
	Abundance (%)	65.2	34.0	0.8	83.9	16.1
Blue Emission	τ (ns)	0.044	0.266	-	0.044	0.239
	Abundance (%)	34.7	65.3	-	59.4	40.6

Figure S1 presents a schematic of the fabrication process of the patterned WO_3 microdisc arrays. The micropatterned arrays of WO_3 were electrochemically deposited on patterned indium tin oxide (ITO) glass, which was prepared using photolithography.

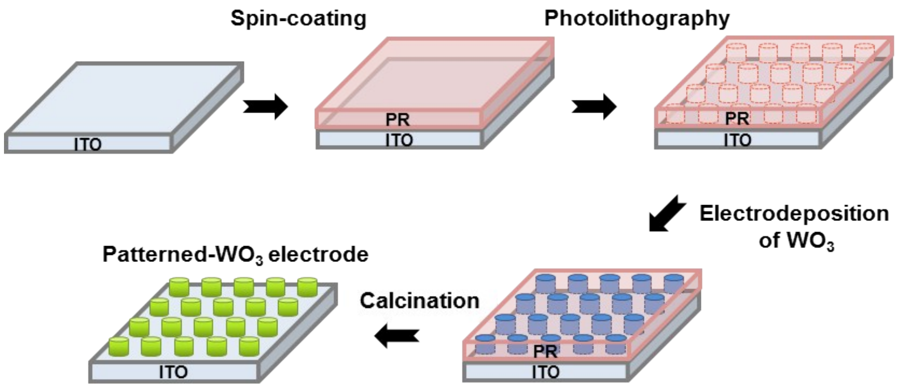

Figure S1. Schematic illustration of fabrication process for the patterned WO_3 microdisc arrays.

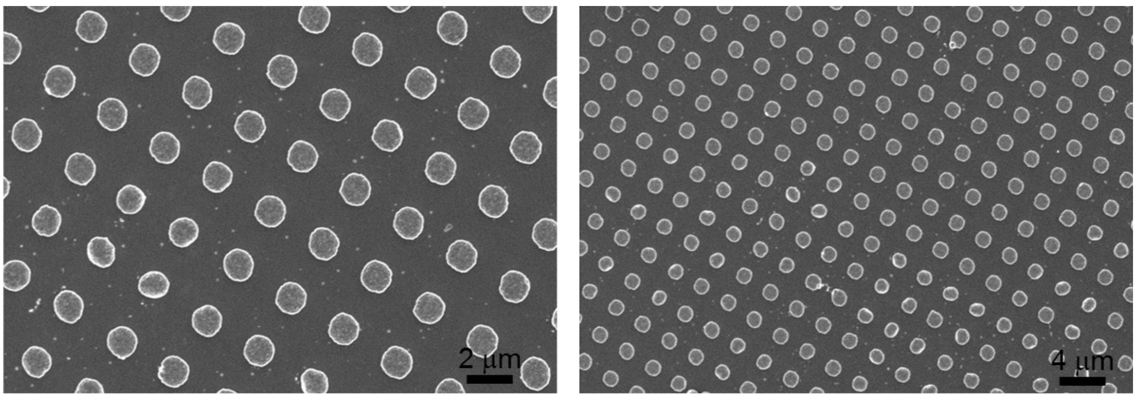

Figure S2. FE-SEM images of WO_3 microdisc arrays electrodeposited on the patterned ITO with 1.5 C of the passed charge.

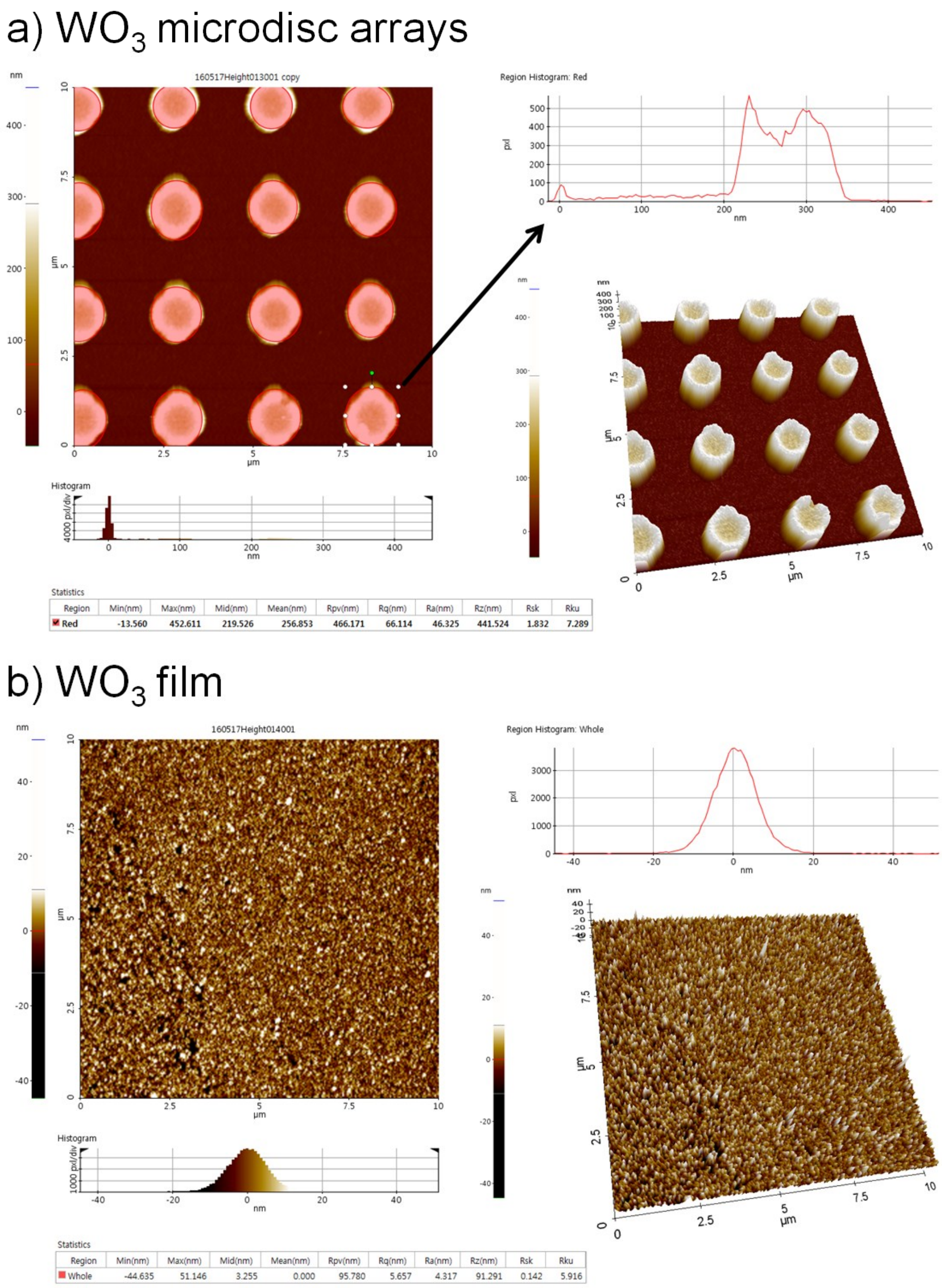

Figure S3. AFM images of (a) WO_3 microdisc arrays and (b) WO_3 film. The images and roughness of samples were obtained using an atomic-force microscopy (AFM, NX20, Park Systems) in non-contact mode. AFM scans were taken over 10 μm × 10 μm areas. The thickness of WO_3 microdisc was around 440 nm, which is well agreed with that estimated with the SEM side view image (Figure S3). The average roughness of WO_3 microdiscs alone was estimated to be 46 nm (R_a) – 66 nm (R_q) because of the central valley of the disc, while that of the entire sample electrode (10 μm × 10 μm) was 96 nm (R_a) – 114 nm (R_q). The roughness of WO_3 film (10 μm × 10 μm) was 4.3 nm (R_a) – 5.7 (R_q). The higher roughness can cause the light-scattering (a negative effect in the absorption) and the re-absorption of the scattered light (a positive effect in the absorption). These two phenomena can offset or minimize the roughness effect on the overall absorption of WO_3 microdisc arrays.

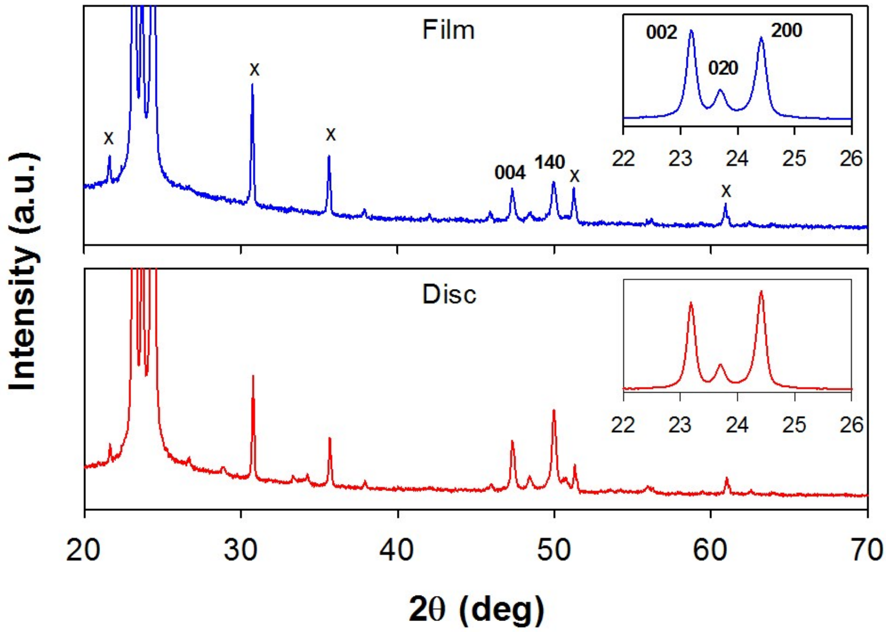

Figure S4. X-ray diffraction patterns of WO_3 film and patterned WO_3 microdisc arrays (x: ITO substrate).

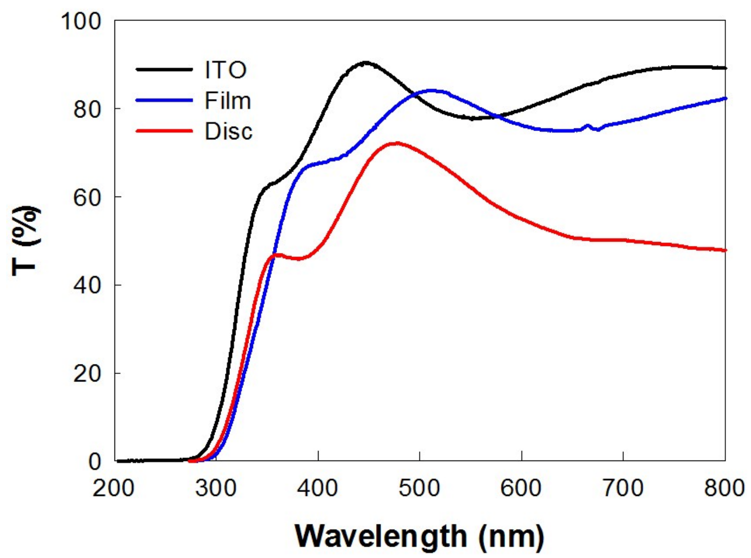

Figure S5. Transmittance of bare ITO substrate, WO_3 film, and patterned WO_3 microdisc arrays.

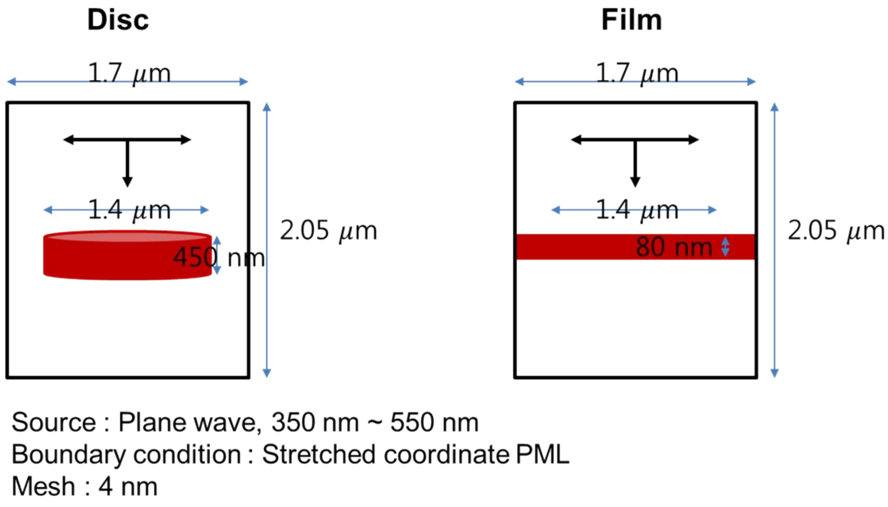

Figure S6. Geometry comparison of WO_3 microdisc and film, and other parameters for finite-difference time-domain simulation.

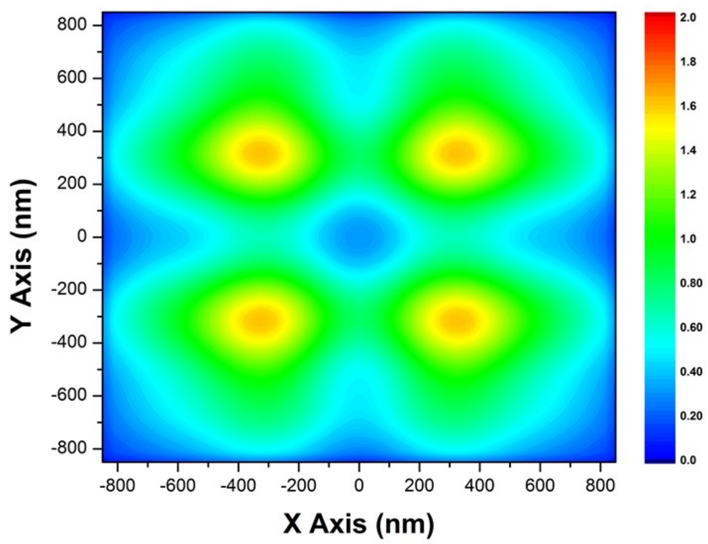

Figure S7. Simulated electric field intensity distribution (top view) for the WO_3 film at 404.7 nm.

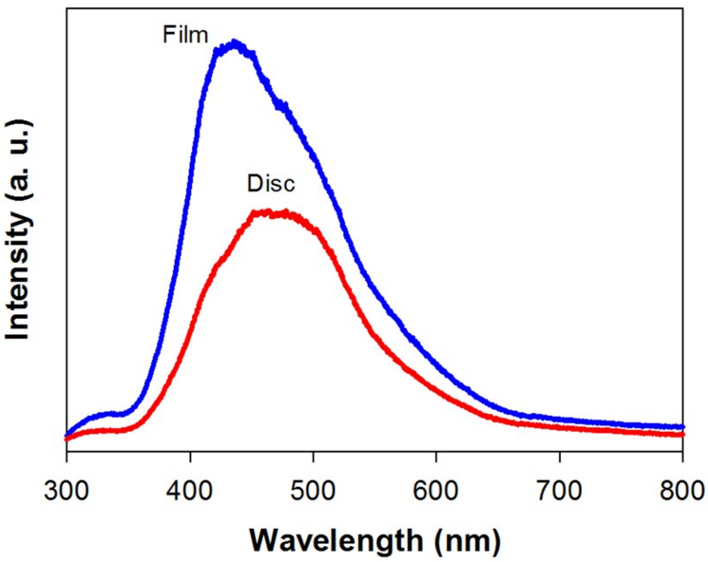

Figure S8. Photoluminescence (PL) emission spectra of WO_3 film and patterned WO_3 microdisc arrays.

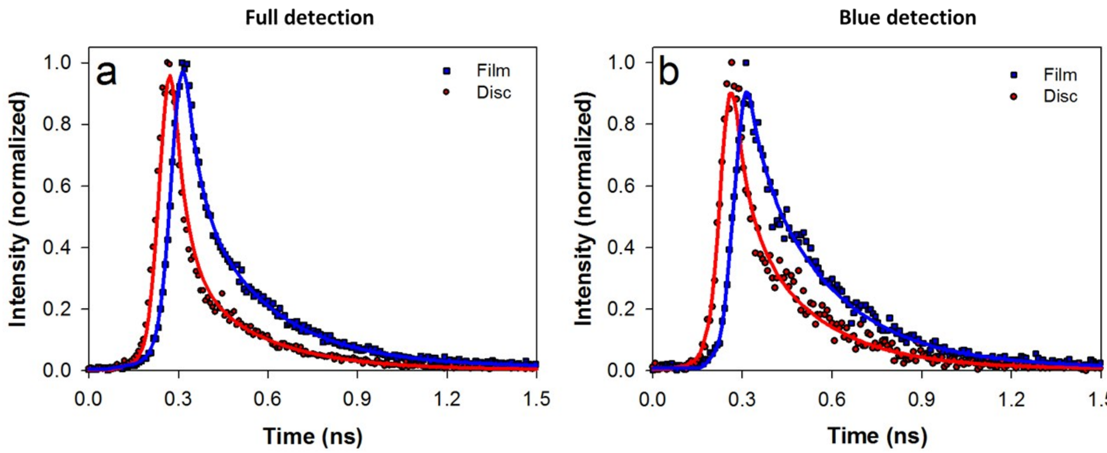

Figure S9. TRPL emission decay of samples (excited at $\lambda = 375$ nm): (a) full range emission and (b) blue emission ($\lambda < 500$ nm).

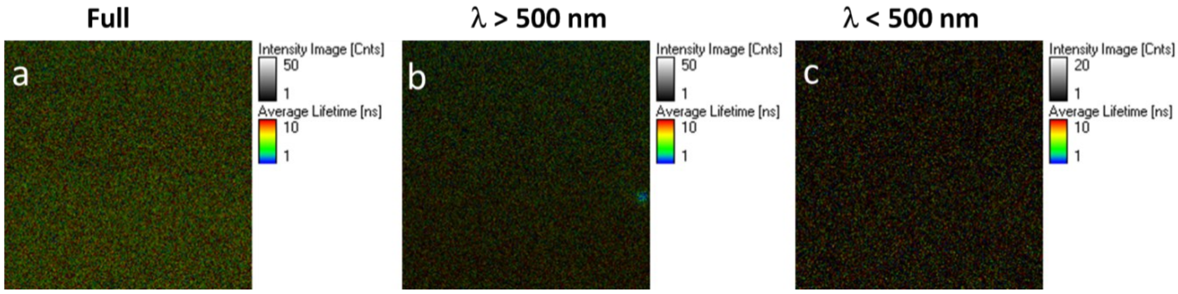

Figure S10. Two-dimensional PL lifetime images for WO_3 film (a: full emission, b: green emission, c: blue emission).

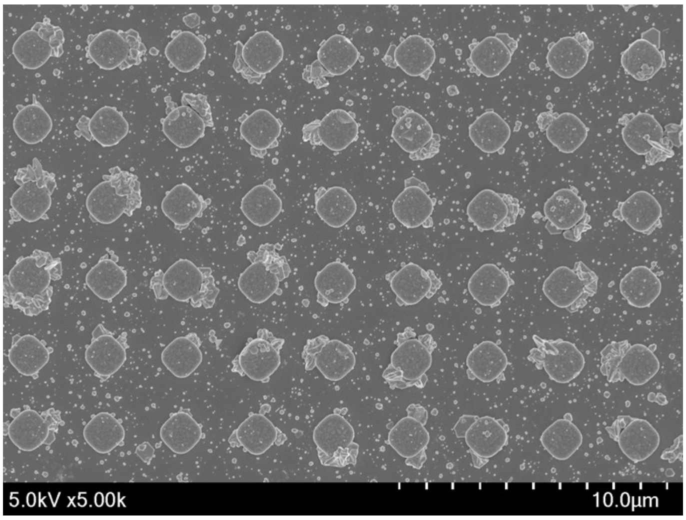

Figure S11. FE-SEM image of Au/WO_3 microdisc arrays prepared by photodeposition of Au for 30 min.

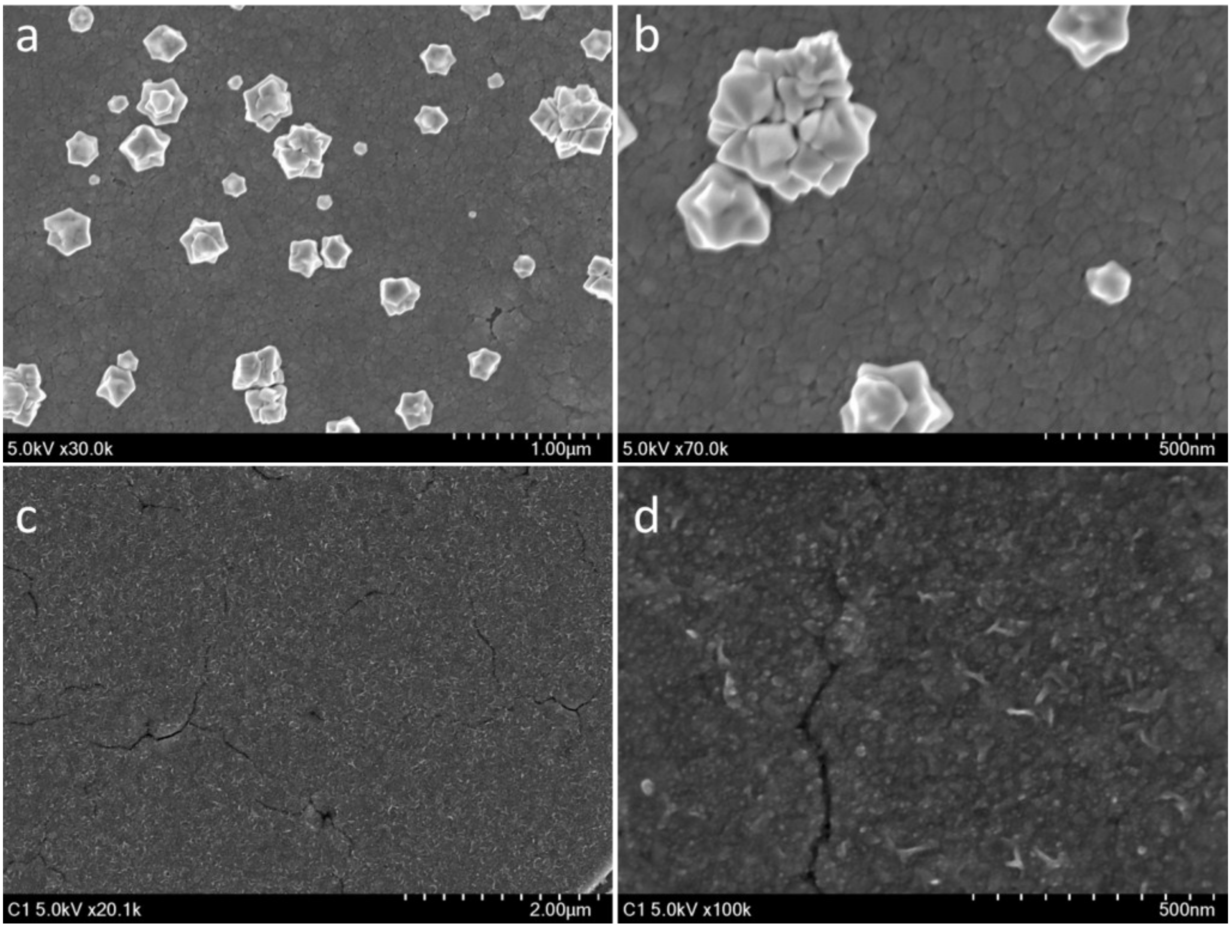

Figure S12. Field-emission scanning electron microscopy images of (a, b) Au/WO_3 film and (c, d) FeOOH/WO_3 film.